sets of parameters. The nuclear potential used was the same as that used by Bjorklund and Fernbach.[1] The shape-elastic curves, calculated with the same parameters, but radii corresponding to the mass numbers 206, 207, and 208 were in all cases essentially the same for each set of parameters. This indicates that the difference which has been experimentally observed is not accounted for by the theory as being due to shape-elastic scattering.

Within experimental error, the angular distribution of the difference is isotropic, as one would expect[7] provided a compound nucleus is formed and the statistical assumption is satisfied. Since the compound-elastic scattering in lead-206 is probably much smaller than in lead-208, we conclude that the major portion of the observed difference is due to compound-elastic scattering in lead-208. If one assumes that the observed difference is due entirely to compound-elastic scattering in lead-208, the total compound-elastic scattering cross section of lead-208 is computed to be 0.8±0.3 barn.

[7] W. Hauser and H. Feshbach, Phys. Rev. **87**, 366 (1952).

ACKNOWLEDGMENTS

We wish to thank Dr. R. G. Moore for making the optical-model calculations, and to acknowledge the invaluable assistance provided by Dr. I. L. Morgan and the Texas Nuclear Corporation staff. We also wish to thank Professor T. W. Bonner and Professor B. B. Kinsey for their advice and criticisms and Professor L. Cranberg for his help in the design of the time-of-flight instrumentation.

PHYSICAL REVIEW VOLUME 116, NUMBER 4 NOVEMBER 15, 1959

Proton-Proton Scattering at 10 Mev*

L. H. Johnston and D. E. Young†
School of Physics, University of Minnesota, Minneapolis, Minnesota
(Received June 22, 1959)

Differential cross sections have been measured for scattering of 9.69-Mev protons by hydrogen gas, covering the laboratory angular range from 45° to 5°. The angular resolution is $\pm\frac{1}{2}°$ at small angles, and estimated absolute probable errors ±0.7% except at the smallest angles. The interference minimum of 51.4 millibarns occurs at 34° c.m. and the 90° cross section is 54.6 mb. The data can be fit with the following set of phase shifts: ${}^1S_0=54°$, ${}^3P_0=+2.83°$, ${}^3P_1=-5.07°$, ${}^3P_2=+2.22°$, ${}^1D_2=+0.2°$.

I. INTRODUCTION

PROTON-PROTON scattering has been done by several authors[1–4] at energies close to 10 Mev Techniques now available permit improved accuracy and permit the measurements to be extended to the small-angle region where the cross section goes through a minimum due to interference of the nuclear phase shifts with the strong Coulomb phase shifts. These interference terms are very sensitive indicators of small amounts of P wave and higher phase shifts.[5] One interesting feature of p-p scattering at this energy (10 Mev) is that the S-wave phase shift seems to go through a maximum value here.[6]

Protons for this experiment were provided by the first accelerating cavity of the Minnesota proton linear accelerator. Excellent collimation was achieved by allowing the 10-Mev beam to "coast" 80 feet through the other two cavities, which were unexcited.

* Supported in part by the U. S. Atomic Energy Commission.
† Now at Midwestern Universities Research Association, Madison, Wisconsin.
[1] James Rouvina, Phys. Rev. **81**, 593 (1951) (7.51 Mev).
[2] B. Cork and W. Hartsough, Phys. Rev. **94**, 1300 (1954). (9.7 Mev).
[3] Allred, Armstrong, Bondelid, and Rosen, Phys. Rev. **88**, 433 (1952). (9.7 Mev).
[4] F. E. Faris and B. T. Wright, Phys. Rev. **79**, 577 (1950). (12.4 Mev).
[5] Pierre Noyes (private communication).
[6] L. H. Johnston and Y. S. Tsai, Phys. Rev. **115**, 1293 (1959).

II. APPARATUS

A. Scattering Chamber

The scattering chamber and most of the techniques used in this experiment are only slightly modified from those used for 40-Mev p-p scattering[7] so here only the modifications will be described.

The general layout of the experiment is identical to Fig. 1, reference 7, and the scattering chamber is shown in Fig. 2, reference 7. Modifications to the scattering chamber were as follows:

1. All collimators and telescope slits were reduced in thickness to 0.032 inch (Brass).
2. The input collimator and entrance foil to the chamber were moved 20 inches downstream to give a shorter path through the scattering gas. This increased the minimum scattering angle from 4° to 5°. The input collimator is circular and has 0.8-cm diameter.
3. The beam entrance foil was changed to $\frac{1}{4}$-mil Mylar and the exit foil to $\frac{1}{2}$-mil aluminized Mylar.

[7] L. H. Johnston and D. A. Swenson, Phys. Rev. **111**, 212 (1958).

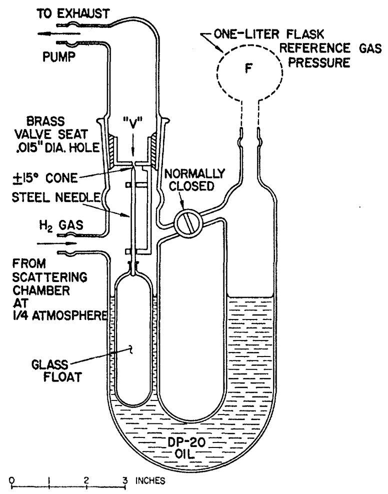

FIG. 1. Pressure-regulating escape valve.

4. The entrance foil to the NaI detector on the 10°–60° telescope was changed to 1-mil aluminized Mylar, while the small-angle telescope detector retained its 2-mil aluminum foil.

5. The angle calibration of the telescopes was re-established with reference to the new collimators and telescope slits. Beam pictures were taken at the position of the Faraday cup, to insure that the chamber was aligned with the beam direction, and that the beam was well contained by the cup.

B. Target Gas

The hydrogen pressure used in this experiment was one-quarter atmosphere, which would have meant that a static gas filling would have been appreciably contaminated in two hours, for runs at small angles. Hence a dynamic gas system was devised. Pure hydrogen was continually let into the chamber from a palladium filter, and the pressure was regulated by allowing the gas to escape from the chamber through the pressure-regulating valve shown in Fig. 1. This valve was found to regulate the pressure to better than one millimeter of oil pressure, or less than 1/10 mm of mercury. The regulating pressure is made proportional

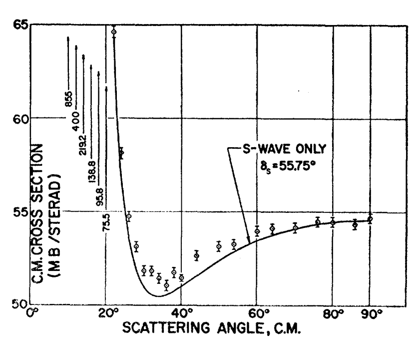

FIG. 2. Angular distribution of p-p scattering cross sections. The theoretical curve is for S-wave phase shift only, chosen to fit the data at 90°.

to the absolute temperature of the room by using a fixed-volume flask (F) of gas as the reference pressure. This maintains the hydrogen in the scattering chamber at constant density in spite of room temperature changes. Temperature and pressure were measured before and after each run as a precaution. The hydrogen pressure was measured by a mercury manometer whose supply line was independent of the gas escape tube leading to the pressure regulating valve.

C. Measurement of Beam Charge

The collector cup system used here was the same one used in the previous 40-Mev experiment.[7] Whereas tests at 40 Mev indicated that the potential on the repeller ring located between the cup and the foil had

TABLE I. Analysis of errors.

Source of error	Absolute error (±)	Relative error (±)
Beam current errors:		
Capacitance	0.2%	0.1%
Voltage	0.1%	0.1%
Electrometer drift	0.1%	0.1%
Charge collection	0.2%	0.0%
Counting errors:		
Nuclear reactions	0.0%	0.0%
Slit scattering	0.1%	0.1%
Counting statistics	0.3%	0.3%
Counting losses	0.1%	0.1%
Background	0.1%	0.1%
Geometrical errors:		
Geometry measurements	0.2%	0.1%
Angle calibration[a]	0.2%	0.1%
Target errors:		
Gas temperature	0.1%	0.1%
Gas pressure	0.1%	0.1%
Gas impurities	0.1%	0.1%
Beam energy errors:		
Mean energy	0.3%	0.1%
Energy dependence On angle	0.0%	0.1%
Total probable errors	0.7%	0.5%

[a] Errors due to angle calibration are as listed, except for the following small angles where they are relatively more important: 5°, 1.6%; 6°, 0.8%; 7°, 0.4%; 8° and larger, 0.2%.

no measurable effect on the charge collection, at 10 Mev it was found that a 4% error resulted if the repeller potential was zero, while the 400 gauss magnetic field was on. The sign of the error corresponds to electrons escaping from the cup. This error became negligible if minus six volts was applied to the ring. To be safe, the potential was made −1000 volts during runs. It was found that the magnetic field made no measurable difference if −1000 volts was on the repeller.

III. ERRORS AND CORRECTIONS

A. Second-Order Geometry

In calculating the cross sections to be attributed to to a given angle, the variation of cross section with angle is treated in terms of the local first and second derivatives.[8] The geometrical formula used for calculating cross sections in the laboratory system of coordinates is

$$C=BN_0\sigma\frac{2v'2v2h}{MR_0\sin\theta}\left\{1+\frac{v^2\cot^2\theta}{3R_0^2}-\frac{v'^2+v^2}{2M^2}+\frac{b^2}{4R_0^2\sin^2\theta}-\frac{3b^2}{8R_0^2}-\frac{h^2}{2R_0^2}+\frac{\sigma'}{\sigma}\frac{\cot\theta}{3}\left(\frac{h^2}{2R_0^2}-\frac{v^2}{MR_0}\right)+\frac{\sigma''}{\sigma}\frac{v^2}{3M^2}\right\},$$

where σ is the laboratory differential cross section and σ' and σ'' are its first and second derivatives with respect to laboratory angle θ. The terms in σ' and σ'' assume that $v=v'$. All other geometrical terminology is that used in reference 7, where the nominal values of the principal dimensions are also given. Conversion to center-of-mass angles and cross sections are performed relativistically, using formulas identical to those given by Chamberlain *et al.*[9]

TABLE II. *p-p* differential cross sections and probable errors for proton laboratory energy = 9.69±0.03 Mev.

θ_{lab}	$\theta_{c.m.}$	$(d\sigma/d\Omega)_{c.m.}$ (mb/sterad)	Absolute probable error ±	Relative probable error ±
5°	10.026°	854.9	1.7%	1.7%
6°	12.031°	400.2	1.0%	0.9%
7°	14.035°	219.2	0.8%	0.6%
8°	16.041°	138.8	0.7%	0.5%
9°	18.046°	95.8	0.7%	0.5%
10°	20.051°	75.5	0.7%	0.5%
11°	22.055°	64.4	0.7%	0.5%
12°	24.060°	58.1	0.7%	0.5%
13°	26.064°	54.7	0.7%	0.5%
14°	28.069°	53.1	0.7%	0.5%
15°	30.074°	51.8	0.7%	0.5%
16°	32.079°	51.8	0.7%	0.5%
17°	34.083°	51.4	0.7%	0.5%
18°	36.087°	51.0	0.7%	0.5%
19°	38.091°	51.7	0.7%	0.5%
20°	40.096°	51.4	0.6%	0.4%
22°	44.103°	52.6	0.7%	0.5%
25°	50.113°	53.1	0.7%	0.5%
27°	54.120°	53.2	0.7%	0.5%
30°	60.128°	53.9	0.7%	0.5%
32°	64.133°	54.05	0.7%	0.5%
35°	70.139°	54.1	0.7%	0.5%
38°	76.144°	54.4	0.7%	0.5%
40°	80.145°	54.4	0.7%	0.5%
43°	86.148°	54.3	0.7%	0.5%
45°	90.148°	54.6	0.7%	0.5%

B. Error Estimates

Table I lists the sources of error considered to be significant with estimates of their magnitudes for affecting the absolute values of the cross section and the relative values. The nature of these errors is discussed in reference 7.

Scattering from detector telescope slits was assumed negligible in this experiment due to the large-scale geometry of the scattering chamber.

Contamination of the hydrogen was shown to be negligible by evacuating the scattering chamber and then allowing it to remain closed off for 12 hours. The scattering yield for the accumulated gases was measured at 5°, where the measured pressure and scattering yield was consistent with assuming the gas to be oxygen or carbon dioxide.

No correction was made for detected protons causing nuclear reactions in the sodium iodide, since this effect amounts to less than 0.1% at 10 Mev.

Small corrections are required by the fact that for different scattering angles the incident beam traverses differing thicknesses of H_2 gas before scattering, which causes small energy changes. This is done assuming a $1/E$ dependence of cross section at angles larger than the interference minimum, and at smaller angles a successively higher power is assumed, ending with $1/E^2$ at 10° c.m.

IV. RESULTS

Calculated cross sections with estimated probable errors are given in Table II. They are plotted in Fig. 2, along with a theoretical curve for pure *S*-wave scattering, chosen to fit the data at 90°.

A phase shift analysis of these data has been made by MacGregor,[10] whose principal results are as follows: The best least-squares fit assuming only *S*-wave scattering gives an *S*-wave phase shift of 56.15°, but the fit is not good, as indicated by the least-squares sum. Good fits can be obtained by including ^3P and $^1D_2$ phase shifts. These fits are not unique, however. He is able to get a continuum of good fits, within limited regions of assumed variation for one of the phase shifts. For example, he can obtain fits for *S*-wave phase shifts anywhere from 52° to 56°. A typical set of phase shifts which fit the data is as follows: $^1S_0=+54°$, $^3P_0=+2.83°$, $^3P_1=-5.07°$, $^3P_2=+2.22°$, $^1D_2=+0.2°$.

The *S*-wave phase shift as a function of energy seems to go through a maximum[6] near this energy; its falling off at higher energies may be taken as evidence for the reality of a repulsive core in the proton-proton potential, which would have a continually greater influence on *S*-wave interactions as they happen at smaller radii.

ACKNOWLEDGMENTS

We gratefully acknowledge the help of Dr. Y. S. Tsai in taking the data for this experiment, and the persistent hard work of the linear accelerator crew.

[8] We are grateful to Professor Richard Hughes for sending us the geometrical calculations of Mr. E. A. Silverstein containing these terms in a readily applicable form. These have now been published by E. A. Silverstein, in Nuclear Instr. 4, 53 (1959).

[9] Chamberlain, Segrè, Tripp, Wiegand, and Ypsilantis, Phys. Rev. **105**, 288 (1957).

[10] M. H. MacGregor, Phys. Rev. **113**, 1559 (1959).